Наносистеми, наноматеріали, нанотехнології
Nanosistemi, Nanomateriali, Nanotehnologii
2025, т. 23, № 1, сс. 109–122
https://doi.org/10.15407/nnn.23.01.0109

PACS numbers: 61.05.cp, 68.37.Ps, 78.20.Ci, 78.66.Li, 81.15.Fg, 81.16.Mk, 81.40.Tv

Effect of Manganese Alloying on the Structural and Optical Properties of Titanium Oxide (TiO_2) Films Prepared by Pulsed Laser Deposition (PLD) Method

Mohammed Ghazi Karim[1] and Reham Zaid Hadi[2]

[1]*Tuz, Salah al-Din, Iraq*
[2]*Faculty of Education,*
Department of Physics,
University of Tikrit,
Tuz Khurmatu, Iraq

The pure membranes of TiO_2 and manganese Mn are prepared in proportions of 5, 3, 1 using the method of pulsed laser deposition (PLD), as the sedimentation process is carried out on glass bases at room temperature, and a thickness of 200 nm; here, the effect of manganese distortion on the structural and optical properties is studied, as the results of x-ray diffraction show that all the membranes are prepared as having a quaternary based structure (tetragonal) as well as within the structural characteristics. The surface topography is studied with an atomic force microscope, and the results show a decrease in the values of surface roughness and mean square root of it with increasing the percentage of distortion; the values of the roughness rate are of 3.935–2.983 nm, but, through visual examinations, it is noted that the values of absorption and absorption coefficient increase with increasing the percentage of distortion, while the optical energy gap decreases with increasing distortion with manganese as 3–2.25 eV.

Чисті мембрани TiO_2 і Манґану Mn були виготовлені в пропорціях 5, 3, 1 за допомогою методу імпульсного лазерного осадження, оскільки процес седиментації проводився на скляних основах за кімнатної температури, та товщиною у 200 нм; тут вивчався вплив спотворення Манґаном на структурні й оптичні властивості, оскільки результати рентґенівської дифракції показують, що всі мембрани, яких було одержано як такі, що мають четвертинну структуру (тетрагональну), а також у межах структурних характеристик. Топографію поверхні досліджували за допомогою атомно-силового мікроскопа, і результати показали зменшення значень шерсткости поверхні та середньоквадратичного значення її зі збільшенням відсотка спотворення; значення рівня шерстко-

сти становили 3,935–2,983 нм, але під час візуальних досліджень було зазначено, що значення поглинання та коефіцієнта поглинання збільшуються зі збільшенням відсотка спотворення, тоді як оптична енергетична щілина зменшується зі збільшенням спотворення з Манґаном як 3–2,25 еВ.

Key words: titanium oxide, jamming, deposition, pulsed laser, optical properties, compositional properties.

Ключові слова: оксид титану, глушіння, осадження, імпульсний лазер, оптичні властивості, композиційні властивості.

(Received 25 October, 2023; in revised form, 13 March, 2024)

1. INTRODUCTION

Thin films are one of the most important newly innovative technologies in materials science and technology [1]. Thin films have a small thickness ranging from several nanometers (nm) to several micrometers (μm) [1, 2].

Thin films are used in a variety of applications, such as medical devices, thin electronics, renewable energy, precision manufacturing and many other fields [3, 4].

Titanium dioxide (TiO_2) membranes have played a large and widespread role in scientific applications due to their great potential in various functional applications such as solar photovoltaics [5], environmental purification [7] and hydrogen production through water splitting [5, 7]. The energy gap of pure TiO_2 oxide provides effective absorption of ultraviolet radiation with a wavelength of less than 400 nm [8], preventing it from obtaining visible light-induced functions [9]. To expand the functions of the visible light region of TiO_2, significant attempts have been made to reduce the bandgap in TiO_2, using non-metallic elements and transition metals as grafting and chopping elements [10].

Titanium oxide (TiO_2) or Titania is one of the most widely used metal oxide semiconductors because it possesses interesting physical and chemical properties. From a technological point of view, this material has the following unique properties: corrosion resistance, non-toxicity, high dielectric constant, high refractive index, high permeability, wide blocked gap, high sensing capabilities, inert surface characteristics, long-term stability and biocompatibility [11, 12].

TiO_2 has found extensive applications in the field of photocatalysis [13], solar cells [14], gas sensors [15], corrosion protective coatings [61], anti-reflective coatings [71], memory devices [81], self-cleaning [91], water treatment [20], antibacterial application [12].

2. WORKING METHOD AND MATERIALS

The used materials are presented in Table 1, which shows the characteristics of these materials.

3. PREPARATION OF MODELS

A sensitive balance of 0.001 of German origin was used to weigh the samples, as a total weight of 2 gm of titanium oxide and manganese was taken, where the percentages of manganese were 1, 3, 5 of the total weight and the rest of the percentage is due to the base material titanium oxide.

After preparing the samples and taking the proportions, the hydraulic press device manufactured by Sky Spring was used; the samples are placed in a mold with a diameter of 12 mm and exposed to high pressure by 5 Tons.

The pressure and time are carefully adjusted to ensure that coherent and homogeneous samples are obtained, and Fig. 1 shows the hydraulic piston device.

TABLE 1. Specifications of the materials used.

Material	Purity	Density, g/cm^3	Company
TiO_2	99.9%	4.5	Titanium industries
Mn	99.7%	7.2	BHP Billiton

Fig. 1. Hydraulic press.

4. SEDIMENTATION PROCESS

After the pressing process, the samples are processed to prepare them for membrane formation, a pulsed laser device of the type of laser Nidemum–Yak shown in Fig. 2 was used, pulsed laser deposition technology was used with a capacity of 500 mJ to heat the surface of the sample tightly and form a thin layer of material on the surface of the glass base with dimensions 50×20×1.2 of Chinese origin. In the laser deposition process, laser parameters such as power, frequency and time are precisely controlled to ensure accurate membrane formation and high quality. Table 2 explain the specifications of the laser device used in the sedimentation process. Using the sampling and laser sampling process, Mn-impregnated titanium oxide samples are prepared to form the membrane and achieve excellent results in manufacturing applications and technical research that require precise, high-quality installations, such as electronic devices, solar panels and optical technologies.

5. THICKNESS MEASUREMENT

Thin film thickness measurement helps to understand the physical properties of membranes and their behaviour. This information can be used to improve membrane design and improve the performance

Fig. 2. UV spectrophotometer.

TABLE 2. Specifications of pulsed laser device used in sedimentation.

Properties	Value
Energy	100–1000 mJ
Wave length	532–1064 nm
Frequency	1–6 Hz

of associated applications. The diffraction method of the laser beam was used to measure the thickness of the prepared membranes using a helium-ion laser source He–Ne, lens and sample, after the laser light passes from the lens to the eye, there will be optical input (which is dark and luminous lines), and the thickness is calculated as follows:

$$d = \frac{\Delta y}{y}\frac{\lambda}{2}, \tag{1}$$

where D means membrane thickness, Δy is the path of laser light deviation y interference hem width, λ—wavelength of helium–neon laser of 632.8 nm.

6. OPTICAL MEASUREMENTS

Optical examinations of titanium oxide membranes with percentages of 1, 3, 5% of manganese were measured using ultraviolet rays using the SP-8001 spectrometer and its wavelength is between 200–1100 nm, and Fig. 2 shows an image of the device used in measuring visual examinations, the sample is highlighted and the amount of light absorbed at a specified wavelength is measured. This measurement can give information about the level of light absorption and changes in the electronic structure of the material, and then through these measurements, we can calculate the rest of the visual examinations such as transmittance, energy gap and reflectivity.

7. STRUCTURAL MEASUREMENTS WITH X-RAYS

X-ray diffraction test was measured for membranes prepared from manganese-tinged titanium oxide, the device was used type 6100Lab X, to perform the x-ray diffraction examination process, the following steps can be carried out:

1) sample preparation of pure manganese-tinged titanium oxide membranes by pulsed laser deposition (PLD) method;

2) the XRD device prepared is properly equipped and set the necessary parameters such as the deviation angle, the deviation range and the appropriate x-ray source;

3) in the x-ray reflexology, x-rays are directed towards the sample and reflected rays are measured; x-rays are guided by control of the angle of deviation and proper recording of reflected rays;

4) the data obtained from the XRD device (Table 3) are analysed using special analysis programs to analyse the results, including comparing the resulting patterns with the approved international databases of known crystal patterns, determining the crystal struc-

ture, and information related to atomic arrangement and distances between crystal layers.

8. ATOMIC FORCE MICROSCOPY

AFM examination is a technique used to analyse and examine surfaces at the atom and particle level. AFM relies on the use of a sensitive needle to interact with the sample surface and measure the forces between them. A small compressive force is applied to the surface using a needle, and by measuring the change in height and interacting forces, a detailed map of the surface is created and various properties are analysed. The atomic force microscopy examination of the prepared membranes was performed using the Bruker dimension icon atomic device force microscope.

9. RESULTS AND DISCUSSION

9.1. Structural Properties

The structural properties of pure manganese-tinged titanium oxide (TiO_2) films were studied by x-ray diffraction technique to know the crystal structural changes of the materials, the crystal size, the homogenization process of the constituent elements of the prepared membranes, the topography of the membranes with the technique of atomic force microscopy, the knowledge of particle roughness and grain size.

9.1. X-Ray Diffraction

The results of an examination using x-ray diffraction technology for pure titanium oxide membranes TiO_2, as titanium oxide appears in the case of pure sample, show through Fig. 3 that the x-ray spectrum of Ti membranes as having a quaternary structure (tetragonal), by observing the diffraction pattern and knowing the locations of peaks of the membranes prepared by pulsed laser deposition method, the appearance of levels (101), (111), (211), (002), (301) and (202). As shown in Table 3, this corresponds to the international card (ASTM) (ICDD) numbered (00-001-1197). After the distortion with manganese, manganese appeared at two levels, namely (210) at the angle 29.547° and (221) at the angle 43.395°, when adding larger percentages of manganese, the intensity of manganese peaks increases and the intensity of titanium oxide peaks decreases, and according to the international card numbered (00-154-1139), the crystal structure of manganese is a cubic structure, but after

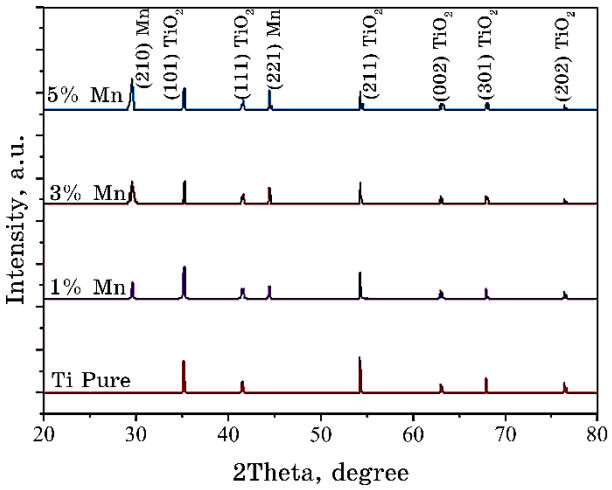

Fig. 3. X-ray diffraction patterns of prepared membranes.

adding it to titanium oxide, it has the same crystal structure as titanium oxide. Consistent with the results of the crystal size, as the crystal size decreases with increasing the percentage of manganese grabbing, and Table 3 shows the results of diffraction of x-rays of membranes prepared from titanium oxide tinged with manganese and for all ratios of distortion, and this is consistent with the findings of the researcher Kharoubi and his group, but they were the crystal size in their study is larger and a slight difference in some peaks and their intensity [22]. Through the results of the x-ray diffraction examination, it was observed that there is crystal growth due to the tendency of titanium oxide peaks to decrease their intensity by adding manganese, which is explained by the crystal growth that occurs during the sedimentation process, and this is consistent with the researcher Bhandarkar and his group [23]. However, in their study, the addition hinders the crystal growth of some peaks as a result of the change in surface energy [24].

9.1.2. Results of Atomic Force Microscopy (AFM)

The study of membranes prepared from manganese-tinged titanium oxide was carried out using atomic force microscopy analysis.

Figure 4 shows pictures of the membranes prepared for pure titanium oxide and tinged with manganese for all proportions, as it can be seen that the nests have a closely homogeneous granular surface and that the surface is very uniform without any cracks.

The AFM image of the sample shows that the addition of manga-

TABLE 3. Test results for x-ray diffraction of the prepared membranes.

Sample	2Theta, deg.	*FWHM*, deg.	C.S., nm	*hkl*	*a*, *b*, *c*; Phase	No. Card
TiO_2 pure	36.102	0.110	90.591	101	$a = b = 4.58$ Å, $c = 2.95$ Å, Tetragonal	No. Card TiO_2 (00-001-1292)
	41.228	0.109	97.947	111		
	54.070	0.204	67.076	211		
	62.160	0.200	86.071	002		
	68.727	0.308	71.947	301		
	76.235	0.413	81.711	202		
1% Mn	29.547	0.142	65.223	210	$a = b = 47.67$ Å, $c = 5.77$ Å, Tetragonal	Crystal system Tetragonal
	36.134	0.192	51.896	101		
	41.175	0.170	62.713	111		
	43.395	0.150	73.614	221		
	54.094	0.261	52.392	211		
	62.950	0.285	61.950	002		No. Card Mn (00-154-1139)
	68.375	0.328	66.517	301		
	76.276	0.495	68.425	202		
3% Mn	29.631	0.178	52.012	210	$a = b = 5.88$ Å, $c = 5.099$ Å	Crystal system Cubic
	36.699	0.290	34.512	101		
	41.280	0.211	50.730	111		
	43.466	0.212	52.256	221		
	54.187	5.901	2.325	211		
	62.791	11.115	1.580	002		
	68.650	6.561	3.362	301		
	76.252	7.680	4.399	202		
	29.446	0.178	51.917	210		
5% Mn	36.397	0.390	25.567	101	$a = b = 8.85$ Å, $c = 9.35$ Å, Tetragonal	
	41.210	0.411	25.993	111		
	43.651	0.312	35.601	221		
	54.372	6.998	1.970	211		
	62.140	11.115	1.546	002		
	68.834	6.981	3.186	301		
	76.124	7.865	4.257	202		

nese on the titanium oxide membranes leads to improved roughness and this is consistent with what the researcher came and this is consistent with the results of the researcher Yang *et al.* [52], as the crystal size began to increase and roughness began to decrease.

These results indicate the process of improvement in the membranes because the increase in roughness reduces the number of self on the surface and collects them to be in the form of larger assem-

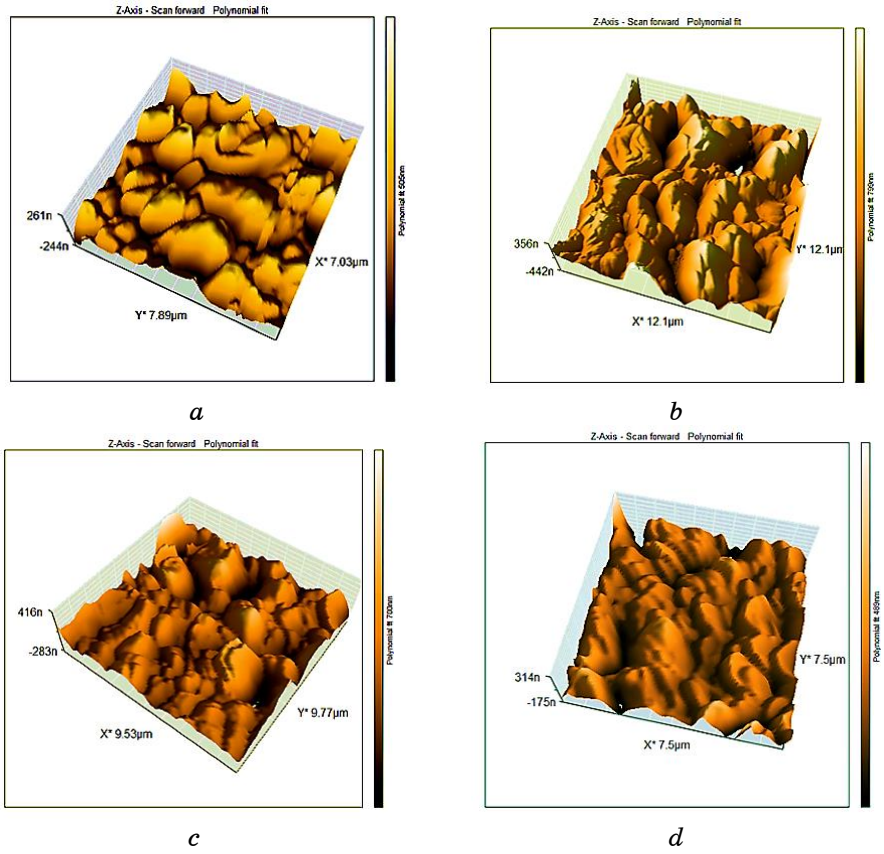

Fig. 4. Atomic force microscopy images of membranes prepared for all alloy ratios: *a*—TiO_2 pure; *b*—1% Mn; *c*—2% Mn; *d*—3% Mn.

TABLE 4. Results of the examination of atomic force microscopy.

Content, %	Average roughness, nm	r.m.s, nm	Average dimeter, nm
TiO_2 pure	3.935	6.981	18.451
1% Mn	3.794	6.036	18.987
3% Mn	3.201	5.249	19.768
3% Mn	2.983	4.780	20.341

blies.

This improvement is due to the effect of manganese on the crystal growth process of titanium oxide membranes and the change in the crystal structure of manganese too because it has a cubic structure as shown in Table 4.

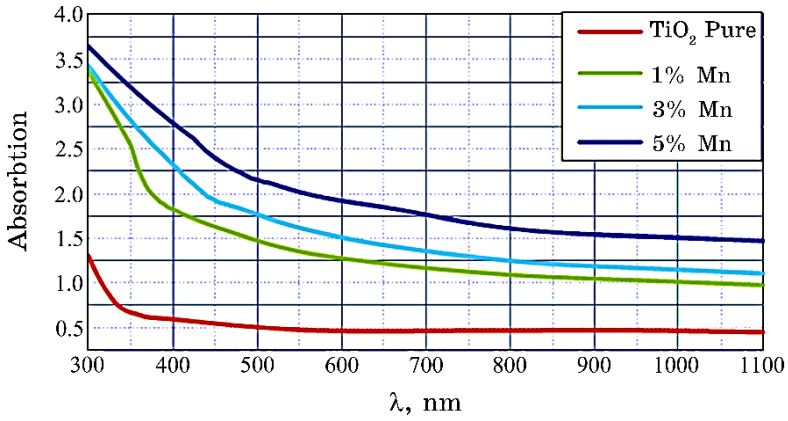

Fig. 5. Absorbency spectrum of titanium oxide membranes.

9.2. Optical Measurements

9.2.1. Absorption

The results of the absorbance values of pure titanium oxide TiO_2 membranes tinged with manganese Mn prepared by pulsed laser deposition decrease with increasing wavelength and the process of distortion with manganese, as Fig. 5 shows that the value of absorbance is the greatest possible at short wavelengths 300 nm and then the absorbance values gradually decrease with increasing wavelength until the absorbance reaches its lowest value at the wavelength 1100 nm, indicating that the membranes The preparation of manganese-tinged titanium oxide has a large absorbency at the visible light area, which makes it suitable in some electronic applications such as solar cells, and decreases with increasing wavelength, and the reason is that the energy of the incident photon is less than the value of the energy gap of the semiconductor and this prevents the electron from moving from the valence beam to the conduction beam [26].The reason for the increase in absorption values with increased manganese distortion ratios is due to the generation of defect sites and thus the creation of additional energy states within the energy band gap. The high concentration of the defect site with the concentration of Mn thus contributes to increased absorption [27].

9.2.2. Absorption Coefficient (A)

Figure 6 shows the relationship between the absorption coefficient and photon energy of membranes prepared by pure pulsed laser

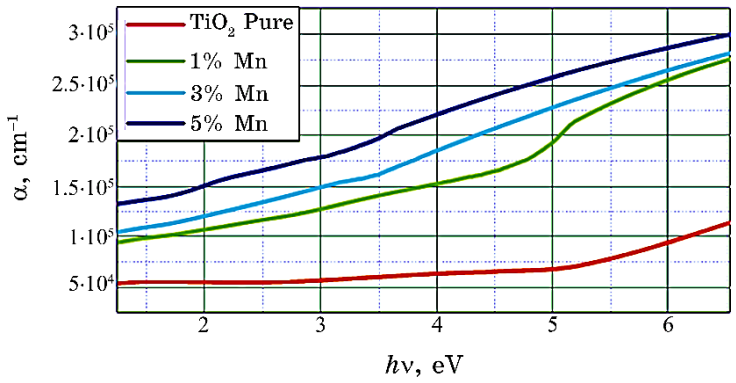

Fig. 6. Relationship between absorption coefficient and photon energy of titanium oxide films.

deposition method with distortion percentages 5, 3, 1. It was found that the values of the absorption coefficient of the membranes are equal to ($\alpha < 10.000$) and this indicates the electronic transfers that occurred are of the type of direct transitions [28]. Through this figure, we notice that the process of morphism with manganese leads to an increase in the values of the absorption coefficient, and this means that the membrane material began to crystallize and homogeneity when it was saturated with manganese and that the process of distortion led to a reduction in crystal defects and a reduction in the levels of localized crystal that exist within the prohibited energy gap that was generated due to defects or defects within the crystal structure, and this is consistent with the researcher [29].

9.2.3. Transmittance

Figure 7 shows the relationship between permeability and wavelength, if the results show there is a decrease in permeability values whenever the percentage of manganese distortion increases as in Fig. 7, titanium oxide membranes have the highest permeability of about 80–90 at room temperature within the visible spectrum region, and Fig. 7 shows the transmittance spectrum with the wavelength of pure titanium oxide membranes tinged with manganese with smearing percentages of 1, 3, 5%. It is noted from the figure that the transmittance decreases with increasing distortion rates, but it begins to increase gradually and for all the prepared membranes when the wavelength increases, and this is consistent with Ref. [30], as the transmittance spectrum of these prepared membranes can be used in the manufacture of the photodetector because

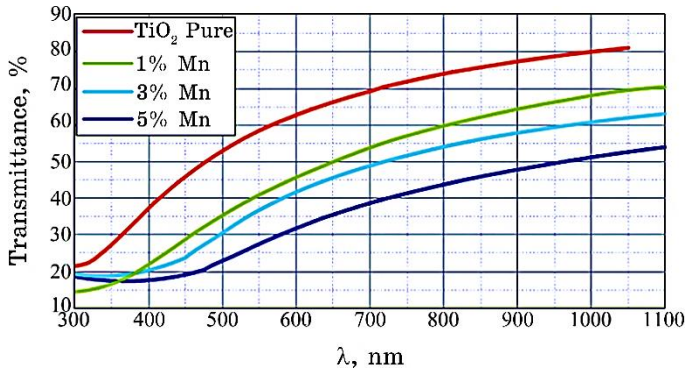

Fig. 7. Permeability spectrometry of prepared titanium oxide membranes.

it is a window to the visible and infrared regions.

9.2.4. Energy Gap

The optical energy gap of the membranes prepared from TiO_2 and pure and tinged with manganese was calculated and a graphical relationship was drawn between $2\alpha h\nu$ with the energy of the incident photon ($h\nu$) as shown in Fig. 8, as this figure shows that the change is linear in a certain range of photon energies (the range of the vis-

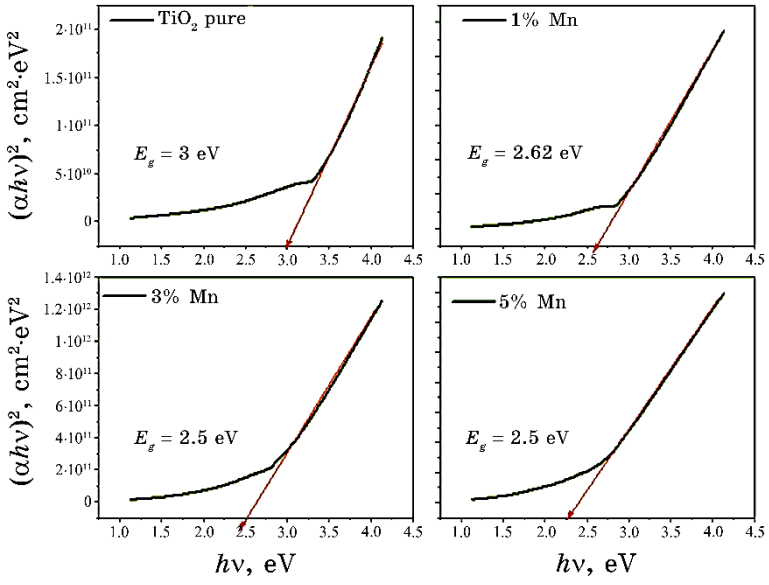

Fig. 8. Energy gap values of prepared titanium oxide membranes.

ible region). The energy gap value of the pure TiO_2 membrane was equal to 3 eV, but when titanium oxide was imbued with manganese, the energy gap began to decrease, and this is consistent with what the researchers came up with Ref. [31], the increase in distortion led to a decrease in the energy gap value from 3 eV for pure membranes to 2.25 eV for the retained membrane showing that the energy gap ratios for all distortion ratios and the reason is due to the presence of surface defects to the tail of the absorption curve [32].

REFERENCES

1. Milton Ohring, *Materials Science of Thin Films. Ch 12. Mechanical Properties of Thin Films* (Academic Press–Elsevier Inc.: 2002), p. 711–781; https://doi.org/10.1016/B978-012524975-1/50015-X
2. Simon M. Sze, Yiming Li, and Kwok K. Ng, *Physics of Semiconductor Devices* (John Wiley & Sons: 2021).
3. Adamo R. Petosa, Deb P. Jaisi, Ivan R. Quevedo, Menachem Elimelech, and Nathalie Tufenkji, *Environmental Science & Technology*, **44**, No. 17: 6532 (2010); doi:10.1021/es100598h
4. Meriem Boudiar, Faouzi Hanini, Abderrahmane Bouabellou, and Yassine Bouachiba, *Journal of Sol–Gel Science and Technology*, **107**: No. 2: 1 (2023).
5. M. N. Leung, D. Y. Leung, and K. Sumathy, *Renewable and Sustainable Energy Reviews*, **11**, Iss. 3: 401 (2007); https://doi.org/10.1016/j.rser.2005.01.009
6. R. D. Tentu and S. Basu, *Curr. Opin. Electrochem.*, **5**: 56 (2017).
7. A. Soussi, A. Ait hssi, L. Boulkaddat, M. Boujnah, K. Abouabassi, R. Haounati, A. Asbayou, A. Elfanaoui, R. Markazi, A. Ihlal, K. Bouabid, N. El Biaze, *Computational Condensed Matter*, **29**: e00606 (2021); doi:10.1016/j.cocom.2021.e00606
8. Swagata Banerjee, Dionysios Dionysiou, and Suresh Pillai, *Applied Catalysis B: Environmental*, **176–177**: 396 (2015); https://doi.org/10.1016/j.apcatb.2015.03.058
9. I. D. Devadoss and S. M. Muthukumaran, *Phys. E: Low-Dimens. Syst. Nanostruct.*, **72**: 111 (2015); https://doi.org/10.1016/j.physe.2015.04.022
10. Ming Yin, Chun-Kwei Wu, Yongbing Lou, Clemens Burda, Jeffrey T. Koberstein, Yimei Zhu, and Stephen O'Brien, *J. Am. Chem. Soc.*, **127**, Iss. 26: 9506 (2005); https://doi.org/10.1021/ja050006u
11. Houda Ennaceri, Mourad Boujnah, Abdelhafed Taleb, Asmae Khaldoun, Rodrigo Sáez-Araoz, Ahmed Ennaoui, Abdallah El Kenz, and Abdelilah Benyoussef, *Int. J. Hydrogen Energy*, **42**, Iss. 30: 19467 (2017); https://doi.org/10.1016/j.ijhydene.2017.06.015
12. A. Arunachalam, S. Dhanapandian, and C. Manoharan, *J. Mater. Sci. Mater. Electron.*, **27**: 659 (2016); https://doi.org/10.1007/s10854-015-3802-9
13. Shuo Wang, Liming Bai, and Xinling Ao, *RSC Adv.*, **8**: 36745 (2018); https://doi.org/10.1039/C8RA06778C
14. A. Arunachalam, S. Dhanapandian, C. Manoharan, and R. Sridhar, *Acta Mol. Biomol. Spectrosc.*, **149**: 904 (2015);

https://doi.org/10.1016/j.saa.2015.05.014
15. Subodh Srivastava, Sumit Kumar, V. N. Singh, M. Singh, and Y. K. Vijay, *Int. J. Hydrogen Energy*, **36**: 6343 (2011); https://doi.org/10.1016/j.ijhydene.2011.01.141
16. A. Elfanaoui, E. Elhamri, L. Boulkaddat, A. Ihlal, K. Bouabid, L. Laanab, A. Taleb, and X. Portier, *Int. J. Hydrogen Energy*, **36**: 4130 (2011); https://doi.org/10.1016/j.ijhydene.2010.07.057
17. Prabitha B. Nair, V. B. Justinvictor, Georgi P. Daniel, K. Joy, K. C. James Raju, David Devraj Kumar, and P. V. Thomas, *Prog. Nat. Sci.: Materials International*, **24**, Iss. 3: 218 (2014); https://doi.org/10.1016/j.pnsc.2014.05.010
18. Alexandre Bayart, Zhen Mian Shao, Anthony Ferri, Pascal Roussel, Rachel Desfeux, and Sébastien Saitzek, *RSC Adv.*, **6**: 32994 (2016); https://doi.org/10.1039/C6RA01225F
19. Nandang Mufti, Ifa K. R. Laila, Hartatiek, and Abdulloh Fuad, *J. Phys. Conf.*, **853**: 012035 (2017); https://doi.org/10.1088/1742-6596/853/1/012035
20. Jianying Shi, Jun Chen, Zhaochi Feng, Tao Chen, Yuxiang Lian, Xiuli Wang, and Can Li, *J. Phys. Chem.*, **111**, Iss. 2: 693 (2017); https://doi.org/10.1021/jp065744z
21. A. Arunachalam, S. Dhanapandian, C. Manoharan, and G. Sivakumar, *Spectrochim. Acta Mol. Biomol. Spectrosc.*, **138**: 105 (2015); https://doi.org/10.1016/j.saa.2014.11.016
22. Abdelmalek Kharoubi, Amar Bouaza, Bedhiaf Benrabah, Abdelkader Ammari, Hadj Benhebal, Belkacem Khiali, and Cherifa Dalache, *Journal of Molecular and Engineering Materials*, **06**, No. 01n02: 1850001 (2018); https://doi.org/10.1142/S2251237318500016
23. S. Asha Bhandarkar, Prathvi, Akshayakumar Kompa, M. S. Murari, Dhananjaya Kekuda, and Rao K. Mohan, *Optical Materials*, **118**: 111254 (2021); https://doi.org/10.1016/j.optmat.2021.111254
24. Ahmed Mahmood and Mandar Chitre, *OCEANS 2015–Genova (Genova, Italy, 2015)*, p. 1; doi:10.1109/OCEANS-Genova.2015.7271550
25. Xiaoyang Yang, Yuxin Min, Sibai Li, Dawei Wang, Zongwei Mei, Jun Liang, and Feng Pan, *Catalysis Science and Technology*, **8**: 1357 (2018); https://doi.org/10.1039/C7CY02614E
26. B. L. Theraja, *Modern Physics* (S. Chandand Company: 1987), p. 170.
27. Mohammad Reza Golobostanfard and Hossein Abdizadeh, *Ceram. Int.*, **38**: 5843 (2012); https://doi.org/10.1016/j.ceramint.2012.04.034
28. A. M. Nawar, N. A. Aal. N. Said, F. El-Tantawy, and F. Yakuphanoglu, *IOSR–Jap*, **6**, No. 4: 17 (2014); https://doi.org/10.9790/4861-06421722
29. N. Najlaa and T. Latif Jamal M. Rzaij, *Journal of University of Anbar for Pure Science (JUAPS)*, **4**, No. 1: 43 (2020); doi:10.37652/juaps.2022.172320
30. D. Komaraiah, E. Radha, J. Sivakumar, M. V. Ramana Reddy, and R. Sayanna, *Opt. Mater.*, **108**: 110401 (2020); https://doi.org/10.1016/j.optmat.2020.110401
31. P. Dulian, W. Nachit, J. Jaglarz, P. Zięba, J. Kanak, and W. Żukowski, *Opt. Mater.*, **90**: 264 (2019); https://doi.org/10.1016/j.optmat.2019.02.041
32. V. R. Akshay, B. Arun, Guruprasad Mandal, and M. Vasundhara, *Phys. Chem. Chem. Phys.*, **21**: 12991 (2019); https://doi.org/10.1039/C9CP01351B